



UNIVERSITÀ DEGLI STUDI DI SALERNO



Dipartimento di
Fisica E.R. Caianiello

Innovative cone beam computed tomography orbit toward quantitative imaging

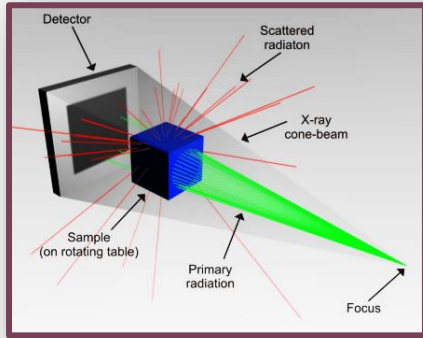
Vanore I.*, Sarno A.

Codice: atticon15180

*i.vanore@studenti.unina.it



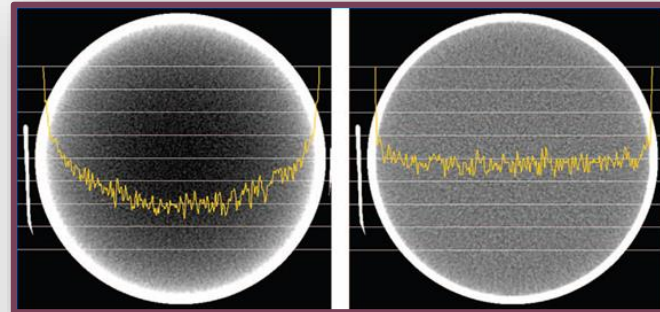
Main CBCT shortcomings



Detected scattered radiation

Leads to low and high frequency noise, reducing accuracy and precision in quantitative evaluation and hiding small details.

Cupping artifact

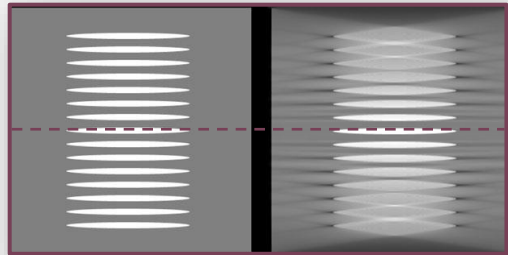


Uniform phantom
with cupping

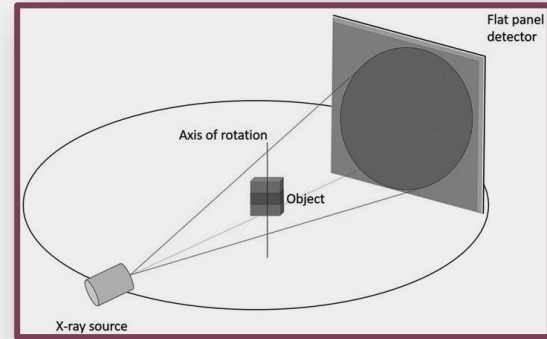
Uniform phantom
without cupping

Main CBCT shortcomings

Cone beam artifacts



Ideal Real
reconstructed slice



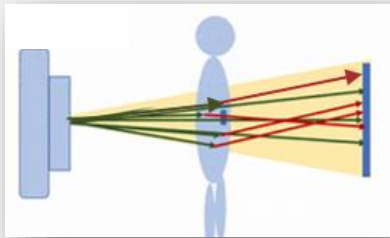
Volumetric beam in a circular orbit

The conventional circular orbit does not satisfy the data sufficiency condition as the distance from the plane containing the source increases.

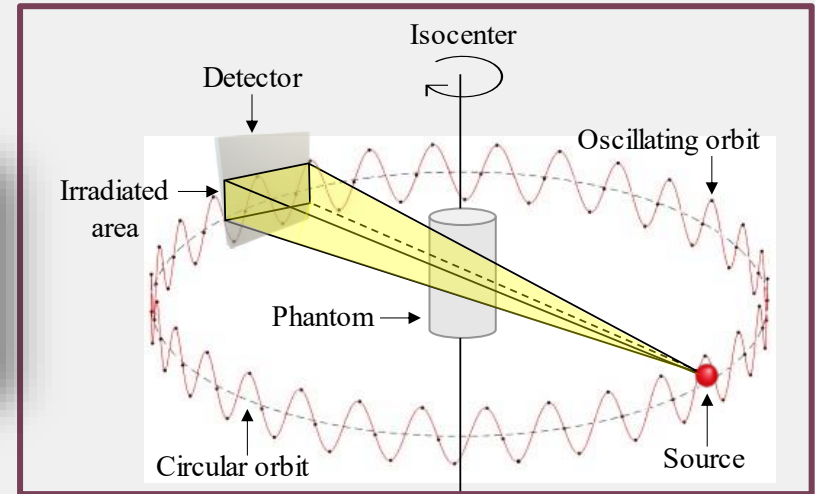
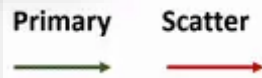
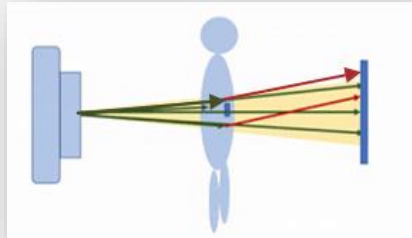
ExoCT scanning protocol

This protocol aims at experimentally study advantages of using a collimated beam and an oscillating scanning geometry for enhancement of quantitative evaluations and visualization of small details in CBCT.

without beam collimation



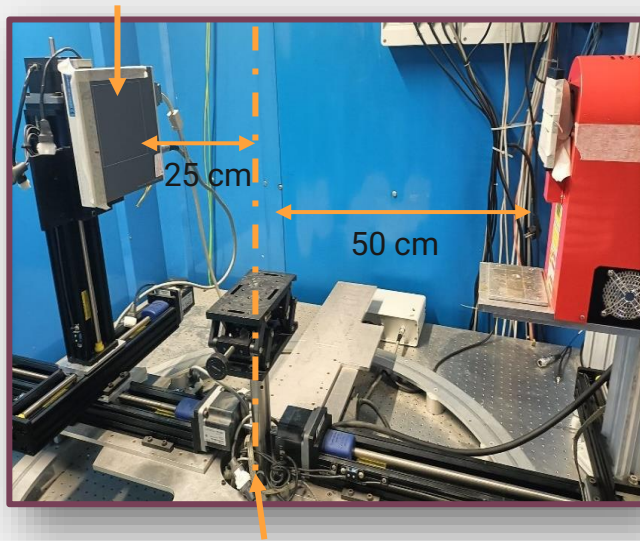
with beam collimation



ExoCT scanning protocol

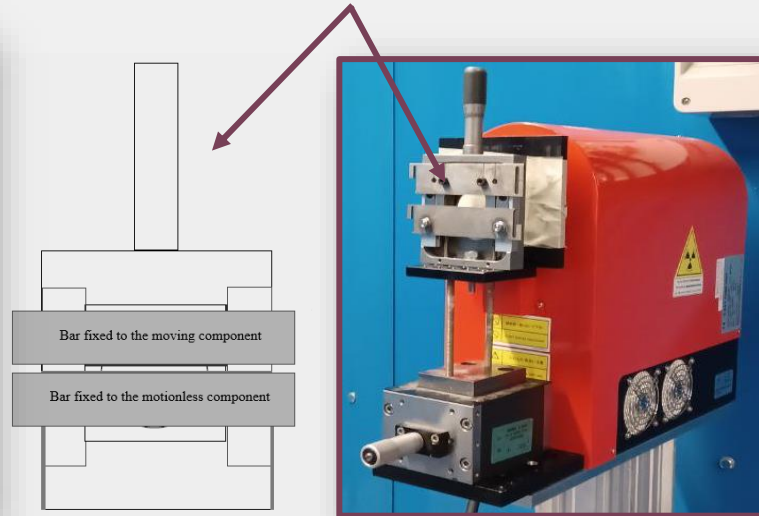
Scatter reduction

Hamamatsu detector C7942CA-02
100 μm pixel pitch



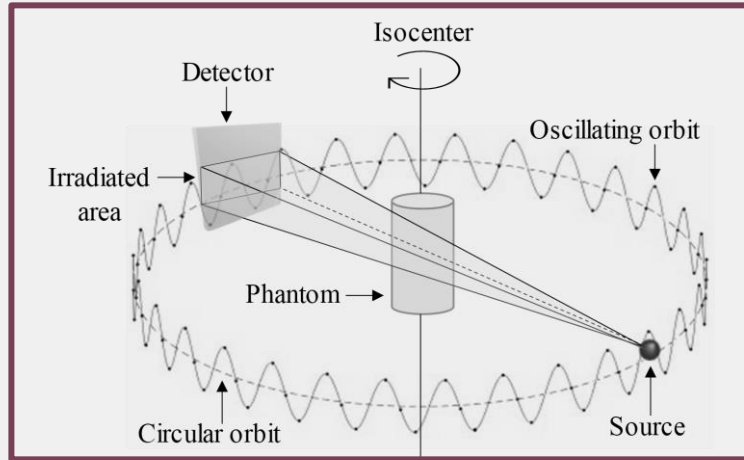
Isocenter

Variable aperture
collimator

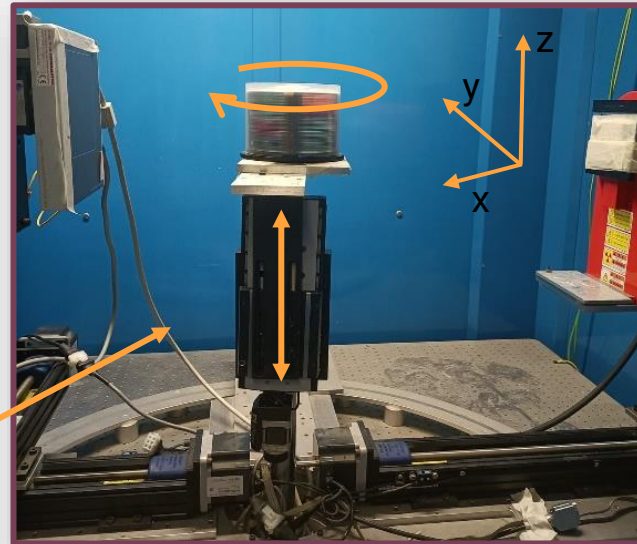


Oscillating orbit

The oscillating orbit is achieved through the relative motion between the sample and the source/detector system.



Gantry circular rotation and phantom motion along the axial direction.

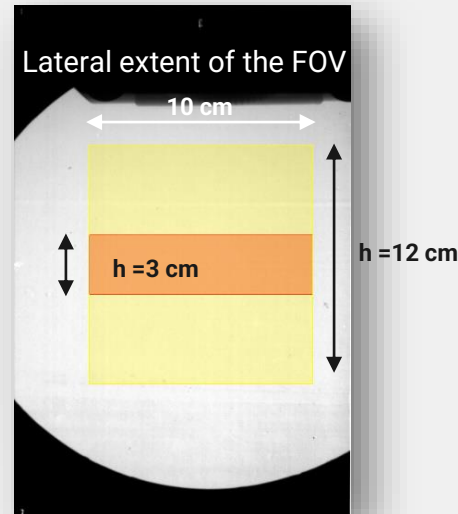


Dosimetric assessment

In order to keep constant the dose in ExoCT with respect to conventional CBCT, a protocol which considers the Kerma Area Product (KAP) as CBCT dosimetric index is applied.



*GafChromic™ XR-QA2 film
calibrated at 80 kV*



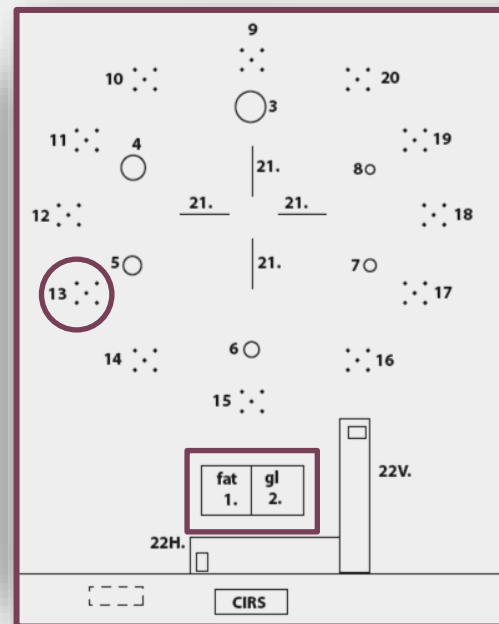
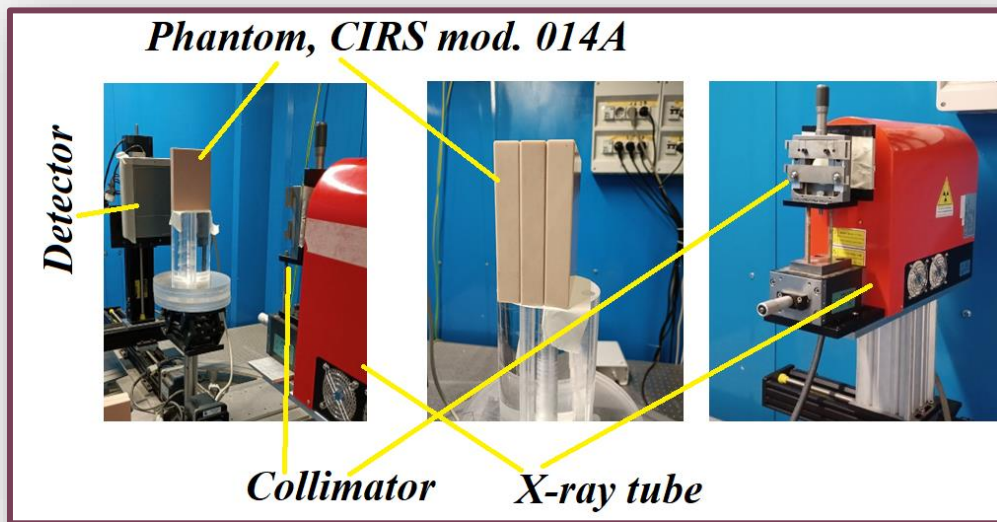
$$I(h) = I(H) \cdot \frac{KAP(H)}{m \cdot KAP(h)}$$

with
 $m \cdot h = H$

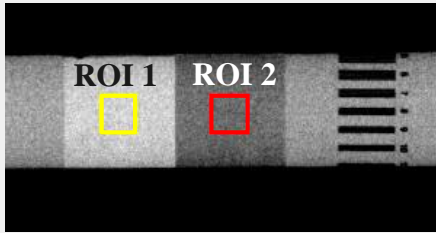
h (cm)	Current (μ A)
12	500
6	498
4	496
3	494
2	490
1	478

2D acquisitions

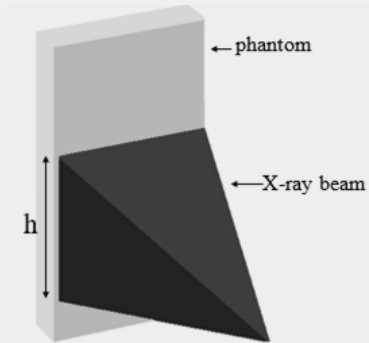
Enhancements on image quality indexes and on microcalcification visibility were evaluated.



2D acquisitions – Scatter influence

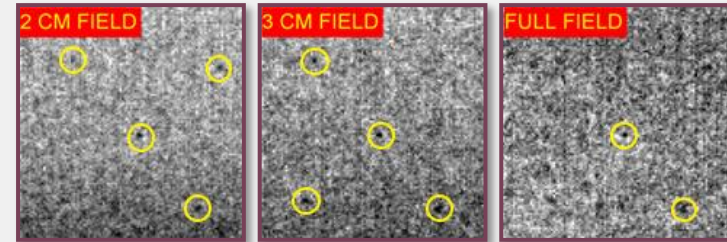
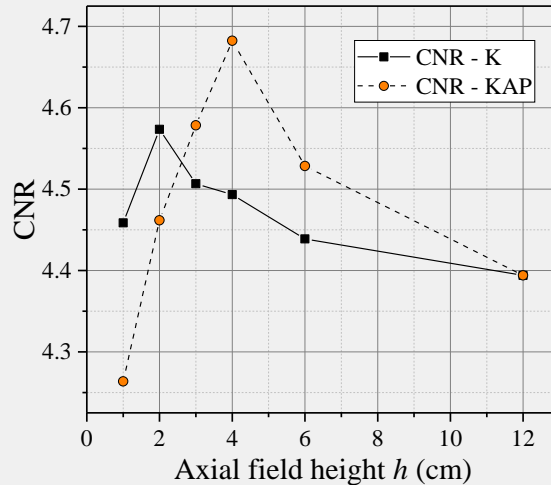


Phantom thickness: 6 cm
 Tube voltage: 80 kV
 Tube current: 500 μ A
 Incident Air Kerma (**K**): 0.5 mGy



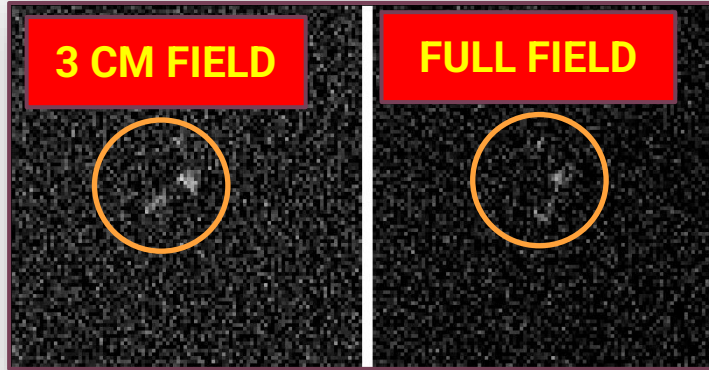
Contrast to Noise Ratio

$$CNR = \frac{\mu_1 - \mu_2}{\sqrt{\frac{\sigma_1^2 + \sigma_2^2}{2}}}$$

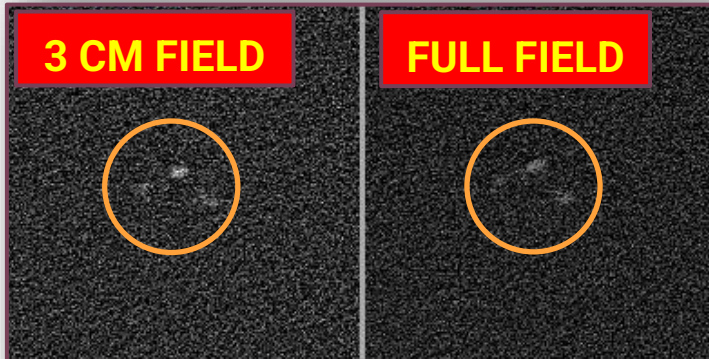


Microcalc. dimension: 160 μ m
 Tube voltage: 80 kV
 Tube current: 200 μ A
 IAK: 5 mGy

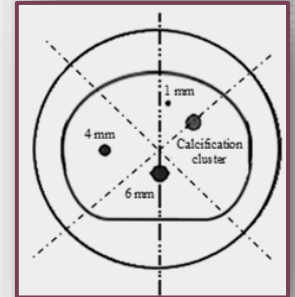
3D acquisitions – Microcalcification visibility



Microcalc. dimension: 300-350 μm
Tube voltage: 80 kV
Tube current: 200 μA
IAK: 10 mGy



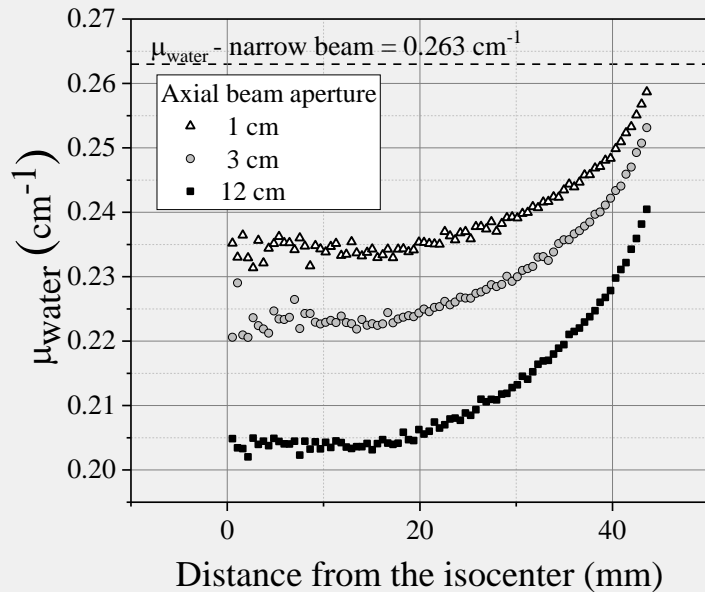
Microcalc. dimension: 300-350 μm
Tube voltage: 60 kV
Tube current: 400 μA
IAK: 12 mGy



Phantom, CIRS
mod. 1272-00-00

3D acquisitions – Cupping artifact

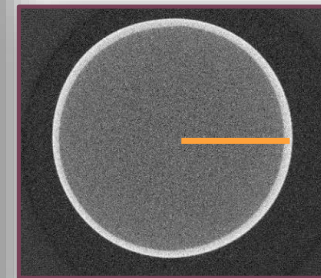
Collimation leads to more uniform attenuation profile of homogeneous objects.



Tube voltage: 80 kV
Tube current: 500 μA



Water phantom



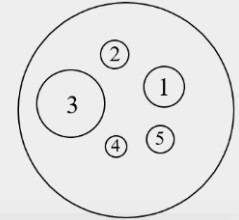
Reconstructed axial slice

3D acquisitions – μ evaluations

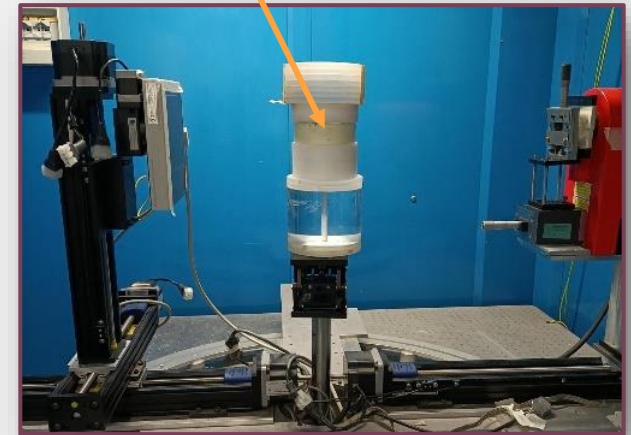
Scatter reduction allows to increase the accuracy in the evaluation of attenuation coefficients μ .

	Difference from expected (%) $h = 12 \text{ cm}$	Difference from expected (%) $h = 3 \text{ cm}$
1. PVC	48.3	33.3
2. PET-P	25.3	14.3
3. TEFLON	42.5	28.7
4. NYLON	20.5	14.3
5. PMMA	26.5	15.0

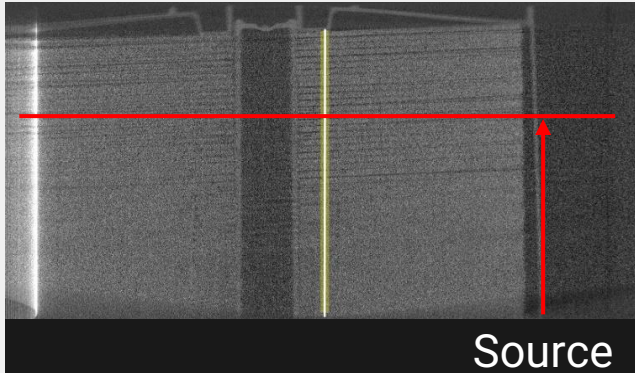
Tube voltage: 80 kV
Tube current: 500 μA



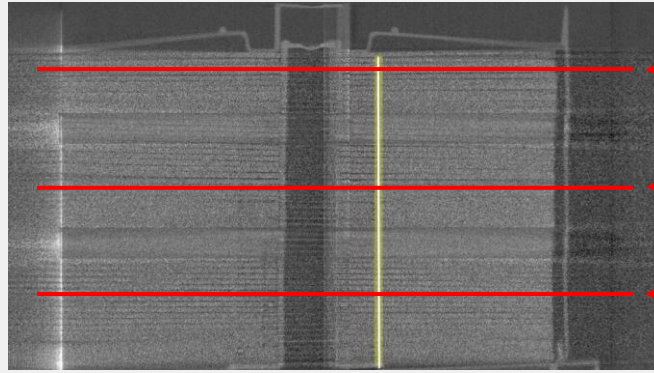
Wax phantom



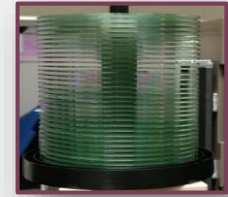
3D acquisitions – CD Defrise phantom



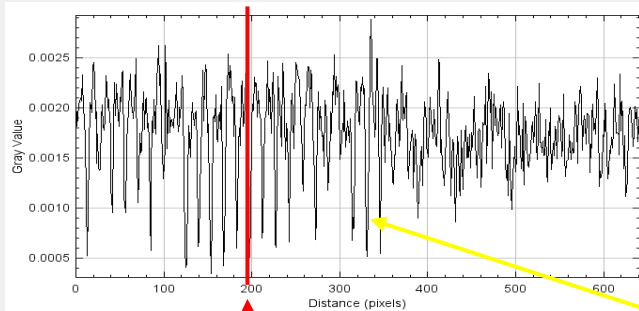
Conventional CBCT



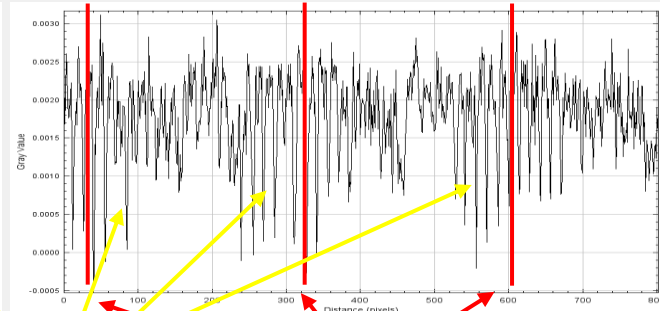
ExoCT



CD Defrise phantom



Source



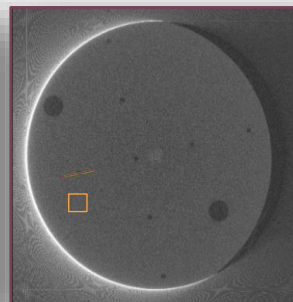
Air gaps

Source

Tube voltage: 80 kV
Tube current: 500 μ A
Axial field height: 33 mm

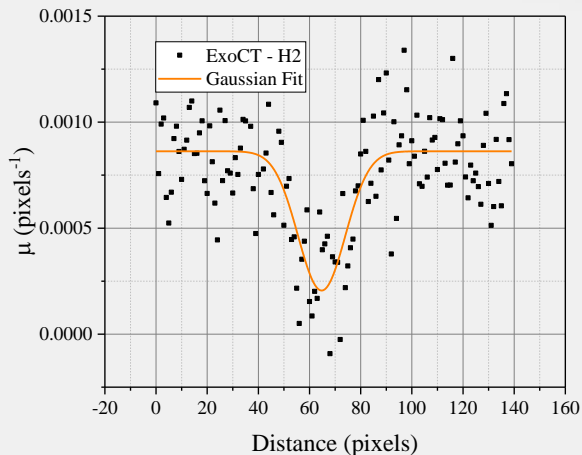
3D acquisitions – PMMA Defrise phantom

Tube voltage: 80 kV
Tube current: 500 μ A
Axial field height: 33 mm

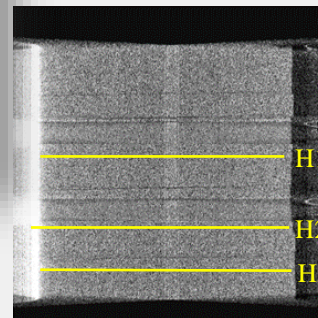


Signal Difference to Noise Ratio

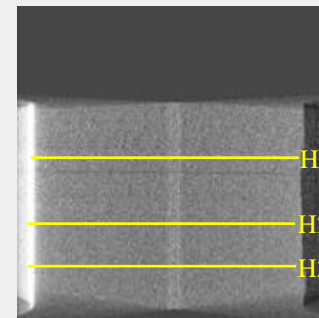
$$SDNR = \frac{\mu_s - \mu_{bgnd}}{\sigma_{bgnd}}$$



PMMA Defrise phantom



ExoCT



CBCT

	Distance from the midplane of CBCT (mm)	SDNR ExoCT	SDNR CBCT
H1	7.1	2.1 \pm 0.2	2.3 \pm 0.2
H2	23.5	2.2 \pm 0.2	1.8 \pm 0.2
H3	38.6	3.2 \pm 0.2	1.7 \pm 0.2

Conclusions

Beam collimation in the axial direction and oscillating scanning geometry result in image quality enhancement with respect to conventional CBCT in terms of:

- Improved visibility of small details both in 2D projections and 3D images;
- Reduced cupping artifacts in 3D reconstructed images;
- Improved accuracy in the evaluation of materials attenuation coefficients in 3D images;
- Improved image conspicuity for field of view portion distant from the plane containing the rotating source.



UNIVERSITÀ DEGLI STUDI DI SALERNO



Dipartimento di
Fisica E.R. Caianiello

**Thank you
for the
attention**

